

Role of hydrodynamic size in colloidal and optical stability of plasmonic Copper nanoparticles

Purnima Sharma^{1,2}, Dinesh Goyal¹, Bhupendra Chudasama² ✉

¹Department of Biotechnology, Thapar Institute of Engineering and Technology, Patiala 147 004, India

²School of Physics and Materials Science, Thapar Institute of Engineering and Technology, Patiala 147 004, India

✉ E-mail: bchudasama@gmail.com

Published in Micro & Nano Letters; Received on 14th March 2019; Revised on 26th June 2019; Accepted on 26th September 2019

Metallic nanoparticles (NPs) exhibit interesting plasmonic characteristics that depend on their size, shape and dielectric medium. Any change in these parameters can lead to significant alternation in plasmonic behaviour of NPs. Plasmonic nanostructures are prepared by wet chemical approaches, which produce NPs with a moderate yield. Amongst plasmonic class of NPs, gold and silver are widely explored in sensors because of their strong plasmon excitation. Copper NPs (CNPs) are gaining increasing attention in plasmonic sensors because of its economic advantages over silver and gold. However, major limitations of these nanostructures are their low yield and poor colloidal stability. In this Letter, authors report scale up of CNPs yield by 100% and studied their colloidal stability in terms of changes in hydrodynamic size and its influence on surface plasmon resonance (SPR). It has been observed that SPR of CNPs is independent of their yield. A gradual decrease in SPR is observed with ageing. This can be attributed to the aggregation-induced microstructural changes in the dispersion. CNPs irrespective of their yield are stable up to 180 days beyond which they lose their colloidal stability and plasmonic properties. Loss of colloidal and plasmonic characteristics of CNPs can be attributed to enhanced hydrodynamic size.

1. Introduction: Metal nanoparticles (NPs) have attracted a lot of attention in past few years due to their unique plasmonic properties [1]. Amongst metals, copper (Cu) because of its antiseptic properties assumes immense importance in biology and medicine since ancient time [2]. Copper NPs (CNPs) show strong antibacterial, antifungal and antifouling characteristics [3, 4]. Apart from these, CNPs have been used in collagen cross-linking and bone formation as well [5]. They are also the potential candidates to replace gold- and silver-based nanostructures in plasmonic sensors.

CNPs are synthesised by variety of chemical methods that include chemical reduction [6–10], microemulsion [11], sonochemical [12], electrochemical [10], thermal reduction [13, 14], pulse laser ablation [15, 16], vacuum vapour deposition [17] and green synthesis [18]. Colloidal stability of NPs synthesised by these routes is an important aspect and has a significant influence on the performance of plasmonic nanostructures. Among these synthesis routes, chemical reduction method is widely explored and most versatile. It is simple, economical and quick approach for NP synthesis. In chemical reduction method, it is possible to control the particle size and shape of CNPs. There are several reports of CNPs synthesis by chemical reduction method. Khaid *et al.* [19] synthesised CNPs by chemical reduction method using ascorbic acid as antioxidant and sodium borohydride (NaBH_4) as a reducing agent and polyvinylpyrrolidone (PVP) as capping agent by adjusting the pH of solution. Synthesised CNPs possess Cu (Cu^0) and cuprous oxide (Cu^{I}) phases. Wu and Chen [20] synthesised metallic CNPs by reduction of cupric chloride with hydrazine using cetyltrimethylammonium bromide (CTAB) as capping agent in inert atmosphere. It is observed that CTAB prevents aggregation of as-synthesised CNPs. Kanninen *et al.* [21] studied the effect of ligand exchange on the stability of CNPs prepared with different capping agents. They have concluded that oleic acid capped NPs showed better stability than the thiols capped NPs.

Dang *et al.* [22] studied the effect of colloidal medium on the stability of CNPs. As-synthesised CNPs were dispersed in water and ethylene glycol. Their stability was evaluated by spectroscopic techniques. CNPs are stable up to 60 days in ethylene glycol, while it precipitates in water after 22 days, indicating CNPs possess better colloidal stability in ethylene glycol. Dang *et al.* [23] have also

studied the colloidal stability of CNPs as a function of reduction time. Maximum stability of 5 days was observed for polyethylene glycol capped CNPs when prepared with a reduction time of 60 min. The surface plasmon resonance (SPR) and oxidation resistance of CNPs show strong dependence on reaction time, pH and relative ratio of surfactant to Cu salt. Li *et al.* [24] have developed a chemical reduction method for the synthesis of uncapped CNPs which are stable for several months. They have also demonstrated that the size and size distribution of CNPs can be controlled by altering the order of addition of chemical reagents in the synthesis. Xiong *et al.* [25] have synthesised 2 nm size CNPs by using L-ascorbic acid as reducing and capping agent. These NPs are stable up to 60 days in aqueous medium and suitable for biomedical applications due to their non-toxic and environmentally friendly reaction medium. Jain *et al.* [26] have studied the effect of reactant concentration and reaction temperature on the morphology, particles sizes and agglomeration of as-synthesised CNPs. Colloids were stable up to 2 months and did not sediment. This Letter also concludes that initial concentration of reactants and reaction temperature has remarkable effect on the particle size and agglomeration of the CNPs.

Although significant work has been done to study the colloidal stability of CNPs, very little information is available on the effect of scale up of NP yield on the colloidal stability of CNPs. Furthermore, the correlation between the colloidal stability and plasmonic properties of CNPs is also not well-understood in the literature. The present work aims to scale up the yield of CNPs (from 200 to 400 mg) without compromising their physical and plasmonic characteristics.

In this Letter, we report the effect of ageing on the colloidal stability of CNPs and its correlation with NPs yield. CNPs were synthesised by chemical reduction method using reducing agents (NaBH_4), antioxidant agent (ascorbic acid), stabilisers and capping agent PVP. As-synthesised CNPs were characterised by ultraviolet–visible (UV–vis) spectroscopy, dynamic light scattering (DLS) and transmission electron microscopy (TEM). Colloidal and plasmonic stability of CNPs was evaluated by monitoring the hydrodynamic size (D_H) through DLS and SPR band through UV–vis spectroscopy as a function of time. Stability of the colloids has also been estimated from these studies.

2. Material and methods

2.1. Materials: Copper chloride, NaBH_4 and PVP (PVP 10,000) were purchased from Sigma-Aldrich. L-ascorbic acid was procured from Merck, India. All chemicals were used as received without any further purification. Aqueous solutions were prepared in Milli-Q water ($\rho=18.2 \text{ M}\Omega$).

2.2. Synthesis of CNPs: Aqueous colloidal dispersions of CNPs were prepared by chemical reduction method [27]. In brief, 5 mM PVP (MW: 10,000) was dissolved in 25 ml warm distilled water under constant magnetic stirring. The requisite quantity of aqueous solution of Cu chloride (1.11 mM) was added into PVP solution and heated at 80°C under constant magnetic stirring. On addition of Cu chloride, the colour of solution changes from yellow to green. To this, 10 mM aqueous solution of NaBH_4 was added dropwise. This changes the solution's colour from green to black. An aqueous solution of ascorbic acid (10 mM) was added to this black solution and allowed to react at 80°C for 5 min. The colour of the colloid changes from black to red indicating the reduction of Cu chloride that leads to formation of CNPs [27]. After this, it was cooled to room temperature. Colloidal dispersion was centrifuged at 6000 rpm for 10 min to remove clusters of CNPs if any. The supernatant containing colloidal dispersion of CNPs was stored at room temperature. Nanoparticle yield for this reaction was 0.2 g. By following the identical protocols, colloidal dispersions of CNPs having NP yield of 0.3 and 0.4 g were also prepared.

2.3. Characterisation of as-synthesised CNPs: As-synthesised CNPs were characterised by UV–vis absorbance spectroscopy, DLS and TEM. UV–vis absorption spectra of CNPs were recorded in the spectral range of 300–700 nm at room temperature on Shimadzu UV-2600 spectrophotometer. Measurements of hydrodynamic particle size and its distribution were performed by the DLS technique. Measurements were carried out on Brookhaven 90Plus particle size analyser. The scattering angle was fixed at 90° . TEM measurements were carried out on Philips CM200 electron microscope operated at 200 kV. Samples for TEM microscopy were prepared by placing a drop of colloidal CNPs on a carbon-coated Cu grid with a mesh size of 200. The aqueous colloid was dried overnight under vacuum. Changes in the plasmonic characteristics [i.e. position of the plasmon resonance band (λ_{SPR}) and its intensity (A_{max})], and hydrodynamic size (D_{H}) of CNPs were tracked over an extended period of 180 days to determine the extent of aggregation in the dispersion and its effect on the colloidal stability and plasmonic properties of CNPs.

3. Results and discussion: As-synthesised CNPs prepared for 0.2 g (sample A), 0.3 g (sample B) and 0.4 g (sample C) yield were characterised by UV–vis spectroscopy, DLS and TEM. The UV–vis absorption spectra of as-synthesised dispersions of CNPs are shown in Fig. 1. A single plasmon resonance band centred at 570–580 nm is observed in the UV–vis spectra of each of the three CNPs dispersions. As can be seen in Fig. 1, irrespective of the CNPs yield, their plasmon bands are similar. This identical plasmonic characteristic of CNPs in the three tested samples indicates the successful scale up of NPs' yield from 0.2 to 0.4 g without any significant deviation in their physical and plasmonic properties. Position of SPR band centred around 570–580 nm is also the characteristic signature of formation of CNPs in Cu^0 state [28]. If CNPs changes their ionic state, a significant blue shift is expected in their plasmon band position [29]. If Cu^0 oxidises to Cu^{2+} (CuO), a plasmon band from 570 to 580 is expected to blue shift to 370 nm, and if Cu^0 oxidises to Cu^{1+} (Cu_2O), the plasmon band is expected to shift to 450 nm [30]. The absence of any additional plasmon absorption bands around 370 and 450 nm indicates that as-synthesised CNPs are primarily in its native metallic Cu^0 state.

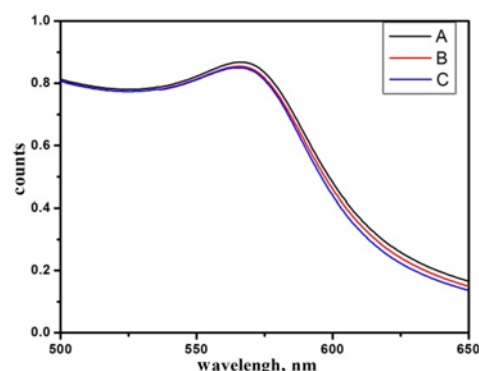


Fig. 1 UV–vis absorption spectra of as-synthesised CNPs (A: 0.2 g, B: 0.3 g and C: 0.4 g yields)

Position of plasmon resonance bands (λ_{SPR}) of as-synthesised CNPs along with their absorption maximum (A_{max}) is summarised in Table 1 for CNPs' dispersions having yields of 0.2 g (sample – A), 0.3 g (sample – B) and 0.4 g (sample – C). The presence of single plasmon resonance band in each spectrum with identical band positions is an indication of the presence of symmetric (spherical) NPs in colloid having similar particle sizes.

Hydrodynamic particle size distribution histograms of as-synthesised CNPs are shown in Fig. 2.

Single size distribution is observed in each histogram. This indicates that NPs are spherical. This observation is in good agreement with the previous assessment of shape of NPs from plasmon

Table 1 Plasmonic and physical characteristics of as-synthesised CNPs

Parameters	Sample A	Sample B	Sample C
yield, g	0.20	0.30	0.40
λ_{SPR} , nm	576.50	572.00	577.50
A_{max}	0.39	0.60	0.74
D_{H} , nm	13.70	11.30	12.10
polydispersity (σ)	0.32	0.30	0.29
particle size, nm	22.8	22.00	23.70

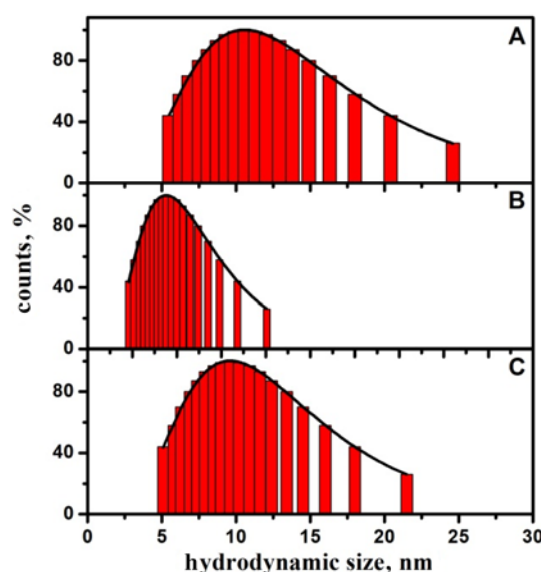


Fig. 2 Hydrodynamic particle size distributions of as-synthesised CNPs (A: 0.2 g, B: 0.3 g and C: 0.4 g yields)

resonance bands observed in Fig. 1 [31]. Each histogram in Fig. 2 is fitted with log-normal particles size distribution function [32]

$$P(D) = \frac{1}{(D\sigma\sqrt{2\pi})} \exp\left[-\frac{(\ln(D/D_0))^2}{2\sigma^2}\right]$$

where σ is the standard deviation, D is the hydrodynamic particle diameter and $\ln D_0$ is the mean of $\ln D$.

The mean hydrodynamic size (D_H) and polydispersity index (σ) thus obtained from the fits are reported in Table 1. The mean hydrodynamic sizes as obtained from the fits for samples A, B and C are identical and ranges between 11 and 14 nm. Their polydispersity (σ) which is a measure of particle size distribution is also similar and ranges between 0.29 and 0.32. Comparable hydrodynamic sizes and polydispersity indexes of all the three dispersions indicate that as-synthesised CNPs have identical physical characteristics.

TEM images of CNPs are shown in Fig. 3 along with their size distribution histograms.

Each histogram is fitted with log-normal particles size distribution function. Mean particle sizes obtained from these histograms are also reported in Table 1. In each TEM, micrographs aggregated NPs with near-spherical morphology can be visualised, which is predicted earlier from UV-vis spectroscopy (Fig. 1) and DLS experiments (Fig. 2). The mean particle size as obtained from the log-normal fit of the particle size distribution histograms ranges between 22 and 24 nm, which is nearly doubled as compared with hydrodynamic particle size (D_H) obtained from DLS. This may be because of heavy clustering of NPs in TEM micrographs, which is making it very difficult to distinguish boundaries of individual NPs.

The colloidal stabilities of as-synthesised CNPs were monitored at periodic intervals of 20 days in terms of SPR peak position by UV-vis spectroscopy and hydrodynamic particle size (D_H) with DLS. The UV-vis spectra of colloids were recorded at periodic intervals over 200 days. The position of SPR bands (λ_{SPR}) and its absorption maximum (A_{max}) as a function of ageing time is shown in Figs. 4 and 5, respectively. A gradual red shift was

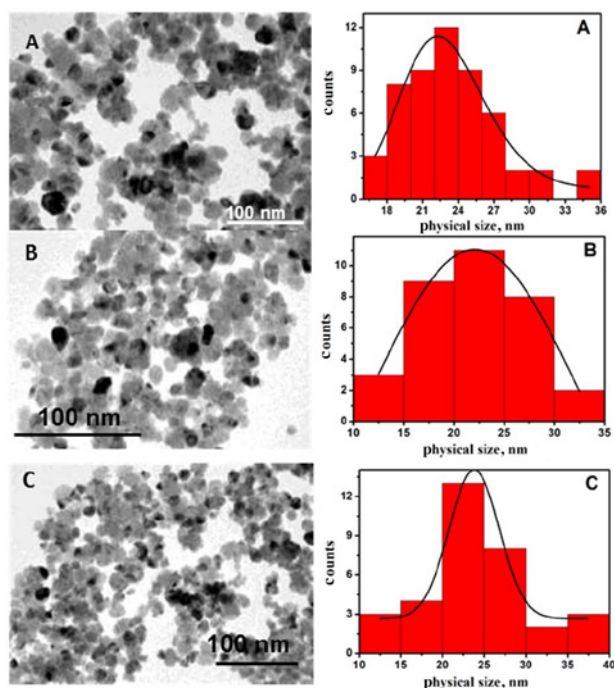


Fig. 3 TEM micrographs and corresponding size distribution histograms of as-synthesised CNPs (A: 0.2 g, B: 0.3 g and C: 0.4 g yields)

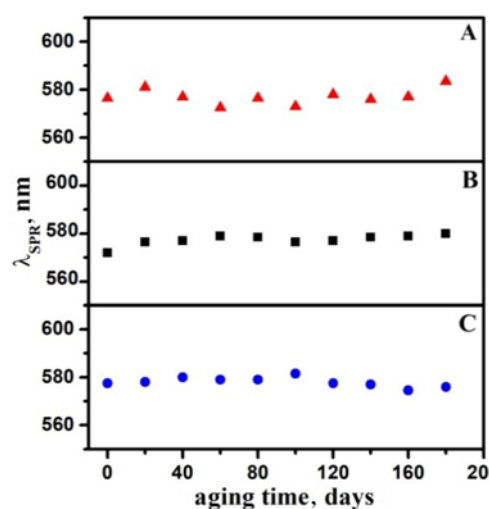


Fig. 4 Effect of ageing on the position of SPR band (λ_{SPR}) of CNPs (A: 0.2 g, B: 0.3 g and C: 0.4 g yields)

observed in the SPR peak position with ageing indicating a possible aggregation or Ostwald ripening of NPs [25]. The mean positions of λ_{SPR} of samples A, B and C are 577.1, 577.4 and 578 nm, respectively. An overall change in the λ_{SPR} position of CNPs is <2% over an ageing period of 180 days. This indicates that irrespective of the yield of NPs, all dispersions show impressive colloidal stability. A gradual decrease in A_{max} of CNPs was observed while ageing (Fig. 5). This might be due to the aggregation of NPs increasing the hydrodynamic particle size of the colloids.

To verify this hypothesis, hydrodynamic particle size (D_H) and the size distribution of CNPs were also observed at periodic intervals of 20–180 days. Each histogram was fitted with log-normal particle size distribution function. From these fits, the mean hydrodynamic sizes of CNPs were determined. Irrespective of the yield of CNPs and time of ageing, each CNPs dispersion show a monomodal particle size distribution indicating that the dispersion contains symmetrical (spherical) NPs. The plot of mean hydrodynamic size of CNPs as a function of ageing time is shown in Fig. 6. Each curve in Fig. 6 is fitted with the following expression:

$$D_H(t) = D_{H0} \exp(t/t)$$

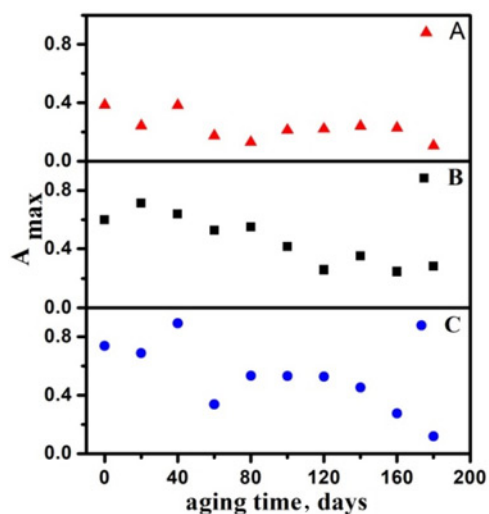


Fig. 5 Effect of ageing on the absorption maximum (A_{max}) of SPR band of CNPs (A: 0.2 g, B: 0.3 g and C: 0.4 g yields)

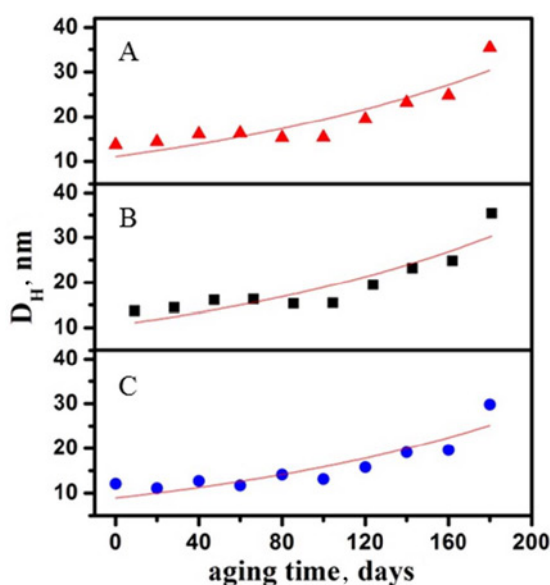


Fig. 6 Effect of ageing on the hydrodynamic particle sizes of CNPs (A: 0.2 g, B: 0.3 g and C: 0.4 g yields)

where $D_H(t)$ is the hydrodynamic particle size of the colloids measured after the ageing for time t , D_{H0} is the hydrodynamic particle size at $t=0$ day and τ represents the shelf life of the colloid. From these fits, the shelf lives of samples A, B and C are determined which are 179, 179 and 174 days, respectively.

As evident from Fig. 6, irrespective of the NP yield (i.e. samples A/B/C), their hydrodynamic particle size increases with ageing. This might be because of the cluster formation in the dispersion caused by desorption of the protective layer of surfactant from the NPs' surface [27]. This gradual increase in the hydrodynamic size with ageing is in good agreement of previous observations of blue shift in SPR peak position and decrease in A_{max} in UV-vis spectroscopy. With ageing, clustering of NPs take place in the dispersion, which results in gradual decrease in the colloidal stability of CNPs. This also led to the decay in the plasmonic performance (A_{max}) of NPs. Colloids lose their dispersion stability beyond 180 days. This decrease in the colloidal stability of CNPs might be due to desorption of the protective layer of surfactant (ascorbic acid) from the surface of CNPs [27].

4. Conclusion: Irrespective of the yield of the CNPs, their hydrodynamic particle size and polydispersity indices are comparable, which indicates that as-synthesised CNPs have identical physical characteristics. With ageing, CNPs lose their colloidal stability and plasmonic properties. Irrespective of the yield or concentration of NPs, dispersions lose their colloidal stability with ageing. Their shelf life is of the order of 180 days. This Letter concludes that effect of ageing on the shelf life of CNPs is independent of NPs' yield and depends only on the surface desorption of surfactant(s).

5. Acknowledgment: Authors are thankful to DST, New Delhi for the FIST – I (SR/FST/PSI-176/2012) programme.

6 References

- Emory S.R., Nie S.J.: 'Screening and enrichment of metal nanoparticles with novel optical properties', *Phys. Chem. B*, 1998, **102**, (3), pp. 493–497
- Kruk T., Szczepanowicz K., Stefanska J., *ET AL.*: 'Synthesis and antimicrobial activity of monodisperse copper nanoparticles', *Colloids Surf. B, Biointerfaces*, 2015, **128**, pp. 17–22
- Cioffi I.N., Torsi L., Ditaranto N., *ET AL.*: 'Copper nanoparticles/polymer composites with antifungal and bacteriostatic properties', *Chem. Mater.*, 2005, **17**, (21), pp. 5255–5262
- Ibrahim N.A., Abo-Shosha H., Gaffar M.A., *ET AL.*: 'Antimicrobial properties of ester-cross-linked cellulose-containing fabrics post-treated with metal salts', *Polym. Plast. Technol. Eng.*, 2006, **45**, (6), pp. 719–727
- Tapeiro H., Townsend D.M., Tew K.D.: 'Trace elements in human physiology and pathology. Copper', *Biomed. Pharmacother.*, 2003, **57**, (9), pp. 386–398
- Cheng X., Zhang H., Yin A., *ET AL.*: 'Modifier effects on chemical reduction synthesis of nanostructured copper', *Appl. Surf. Sci.*, 2006, **253**, (5), pp. 2727–2732
- Pulkkinen P., Shan J., Leppanen K., *ET AL.*: 'Poly (ethyleneimine) and tetraethylenepentamines as protecting agent for metallic copper nanoparticles', *Appl. Mater. Interfaces*, 2009, **1**, (2), pp. 519–525
- Zheng Q.L., Yang Z.M., Ding B.J., *ET AL.*: 'Preparation of copper nanoparticles by chemical reduction method using potassium borohydride', *Trans. Nonferrous Metals Soc.*, 2010, **20**, (1), pp. 240–244
- Khanna P.K., More P., Jawalkar J., *ET AL.*: 'Synthesis of hydrophilic copper nanoparticles: effect of reaction temperature', *J. Nanoparticle Res.*, 2009, **11**, (4), pp. 793–799
- Wei Y., Huaqing X., Lifei C., *ET AL.*: 'Synthesis and characterization of monodispersed copper colloids in polar solvents', *Nanoscale Res. Lett.*, 2009, **4**, (5), pp. 465–470
- Lisiecki I., Pileni M.P.: 'Synthesis of copper metallic clusters using reverse micelles as microreactors', *J. Am. Chem. Soc.*, 1997, **115**, (10), pp. 3387–3397
- Kumar R.V., Mastai Y., Diamant Y., *ET AL.*: 'Sonochemical synthesis of amorphous Cu and nanocrystalline Cu₂O embedded in a poly-aniline matrix', *J. Mater. Chem.*, 2001, **11**, (4), pp. 1209–1213
- Dhas N.A., Raj C.P., Gedanken A.: 'Synthesis, characterization and properties of metallic copper nanoparticles', *Chem. Mater.*, 1998, **10**, (5), pp. 1446–1452
- Naisari M.S., Fereshteh Z., Davar F.: 'Synthesis of oleylamine capped copper nanocrystal via thermal reduction of new precursor', *Polyhedron*, 2009, **28**, (1), pp. 126–130
- Yeh M.S., Yang Y.S., Lee Y.P., *ET AL.*: 'Formation and characterization of Cu colloids from CuO powder by laser irradiation in 2-propanol', *J. Phys. Chem. B*, 1999, **103**, (33), pp. 6851–6857
- Maurizio M.M., Cristina G., Emilia G.: 'Surface-enhanced Raman scattering from copper nanoparticles obtained by Laser ablation', *J. Phys. Chem. B*, 2011, **115**, (12), pp. 5021–5027
- Liu Z., Bando Y.: 'A novel method for preparing copper nanorods and nanowires', *Adv. Mater.*, 2003, **15**, (4), pp. 303–305
- Sastry A.B.S., Aamanchi R.B.K., Prasad C.R.L., *ET AL.*: 'Large-scale green synthesis of Cu nanoparticles', *Environ. Chem. Lett.*, 2013, **11**, (2), pp. 183–187
- Khaid H., Shamaila S., Zafar N.: 'Synthesis of copper nanoparticles by chemical reduction method', *Sci. Int.*, 2015, **27**, (4), pp. 3085–3088
- Wu S.H., Chen D.H.: 'Synthesis of high concentration of Cu nanoparticles in aqueous CTAB solution', *J. Colloid Interface Sci.*, 2004, **273**, (1), pp. 165–169
- Kanninen P., Johans C., Merta J., *ET AL.*: 'Influence of ligand structure on the stability and oxidation of copper nanoparticles', *J. Colloid Interface Sci.*, 2008, **318**, (1), pp. 88–95
- Dang T.M.D., Le T.T.T., Fribourg E.B., *ET AL.*: 'The influence of solvents and surfactants on the preparation of copper nanoparticles by a chemical reduction method', *Adv. Nat. Sci. Nanosci. Nanotechnol.*, 2011, **2**, (1), pp. 025004–025011
- Dang T.M.D., Le T.T.T., Fribourg E.B., *ET AL.*: 'Synthesis and optical properties of copper nanoparticles prepared by chemical reduction method', *Adv. Nat. Sci. Nanosci. Nanotechnol.*, 2011, **2**, (1), pp. 105009–105015
- Li M., Xiang K., Luo G., *ET AL.*: 'Preparation of monodispersed copper nanoparticles by an environmentally friendly chemical reduction', *Chin. J. Chem.*, 2013, **31**, (10), pp. 1285–1289
- Xiong J., Wang Y., Xue Q., *ET AL.*: 'Synthesis of highly stable dispersions of nanosized copper nanoparticles using L-ascorbic acid', *Green Chem.*, 2011, **13**, (8), pp. 900–904
- Jain S., Jain A., Devra V.: 'Experimental investigation on the synthesis of copper nanoparticles by chemical reduction method', *Int. J. Sci. Eng. Res.*, 2014, **5**, (11), pp. 973–978
- Khurana C., Sharma P., Pandey O.P., *ET AL.*: 'Synergistic effect of metal nanoparticles on the antimicrobial activities of antibiotics against biorecycling microbes', *J. Mater. Sci. Technol.*, 2016, **32**, (6), pp. 524–532
- Guajardo-Pacheco M.J., Morales-Sanchaz J.E., Hernandez J.G., *ET AL.*: 'Synthesis of copper nanoparticles using soybean as a chelant agent', *Mater. Lett.*, 2010, **64**, (12), pp. 1361–1364

- [29] Hauman J.L.C., Sato K., Kurtia S., *ET AL.*: 'Copper nanoparticles synthesis by hydroxyl ion-assisted alcohol reduction for conducting links', *J. Mater. Chem.*, 2011, **21**, (20), pp. 7062–7069
- [30] Hu M., Chen J., Li Z.Y., *ET AL.*: 'Gold nanostructures: engineering their plasmonic properties for biomedical properties', *Chem. Soc. Rev.*, 2006, **35**, (11), pp. 1084–1094
- [31] Pal S., Tak Y.K., Song J.M.: 'Does antibacterial activity of silver nanoparticles depends on the shape of nanoparticles? A study of Gram-negative Bacteria *Escherichia coli*', *Appl. Environ. Microbiol.*, 2007, **73**, (6), pp. 1712–1720
- [32] Khurana C., Vala A.K., Andhariya N., *ET AL.*: 'Antibacterial activity of silver: the role of hydrodynamic particle size at nanoscale', *J. Biomed. Mater. Res. A*, 2014, **102**, (10), pp. 3361–3368